Volatile Electrical Switching and Static Random Access Memory Effect in a Functional Polyimide Containing Oxadiazole Moieties

Yi-Liang Liu,[†] Kun-Li Wang,[‡] Guo-Syun Huang,[‡] Chun-Xiang Zhu,[§] Eng-Soon Tok,[⊥] Koon-Gee Neoh,[†] and En-Tang Kang*,[†]

[†]*Department of Chemical & Biomolecular Engineering, National University of Singapore, Kent Ridge, Singapore 119260,* [‡]*Department of Chemical Engineering & Biotechnology, National Taipei University of Technology, Taipei 10608, Taiwan,* [§]*SNDL, Department of Electrical & Computer Engineering, National University of Singapore, Kent Ridge, Singapore 119260, and* [⊥]*Department of Physics, National University of Singapore, Kent Ridge, Singapore 117542*

A solution-processable functional polyimide, P(BPPO)-PI, containing oxadiazole moieties (electron donors) and phthalimide moieties (electron acceptors) was synthesized. A switching device, based on a solution-cast thin film of P(BPPO)-PI sandwiched between an indium−tin oxide (ITO) bottom electrode and an Al top electrode, exhibits two accessible conductivity states and can be switched from the low-conductivity (OFF) state to the high-conductivity (ON) state when swept positively or negatively, with an ON/OFF current ratio on the order of 1×10^4. The device exhibits ON state "remanence", with the ON state retainable for a period of about 4 min after turning off the power. The ON state can be electrically sustained either by a refreshing voltage pulse of −1 V or by a continuous bias of −1 V. The "remanent" but volatile nature of the ON state and the ability to write, read, and sustain the electrical states with bias are characteristic features observed in a static random access memory (SRAM). The mechanisms associated with the memory effect were elucidated from molecular simulation results and changes in the photoelectronic spectrum of P(BPPO)-PI film when the device was switched between the ON and OFF states.

1. Introduction

Over the years, electroactive organic and polymeric materials have been of interest as alternatives to traditional inorganic semiconductor materials for application in electronic memory devices.[1−5] In comparison to inorganic materials-based memory devices, molecular and polymeric memories exhibit low-cost potential, simplicity in structure, good scalability, potential for high-density data storage in 3D arrays, and possibility of fabricating flexible devices.[6] Instead of information storage and retrieval by encoding "0" and "1" as the amount of charges stored in a silicon-based device, polymer electronic memories store data in another form, for instance, based on the high- and low-conductivity response to an applied voltage. In the recent fine works on polymer-based memory devices, polymers were employed as polyelectrolytes[7,8] and as matrices for metal nanoparticles,[9] fullerene,[10,11] and carbon nanotubes[12] in doped or composite systems. The design and synthesis of processable polymers that can provide the necessary electronic properties within a single macromolecule and still possess good chemical, mechanical, and morphological properties is desirable for memory device applications.[13] The materials, device, and mechanism aspects of polymer electronic memories have recently been reviewed.[14]

Polyimides have been widely adopted as insulating or dielectric materials in electrical and electronic devices because of their good thermal stability, good processability, and superior dielectric and mechanical properties.[15] Polyimides have also been investigated

*To whom all correspondence should be addressed. Tel: 65-6516-2189. Fax: 65-779-1936. E-mail: cheket@nus.edu.sg.

(1) Das, B. C.; Pal, A. J. *ACS Nano* **2008,** *2,* 1930–1938.
(2) Tseng, R. J.; Baker, C. O.; Shedd, B.; Huang, J. X.; Kaner, R. B.; Ouyang, J. Y.; Yang, Y. *Appl. Phys. Lett.* **2007,** *90,* 053101.
(3) Rath, A. K.; Dhara, K.; Banerjee, P.; Pal, A. J. *Langmuir* **2008,** *24,* 5937–5941.
(4) Yonekuta, Y.; Susuki, K.; Oyaizu, K.; Honda, K.; Nishide, H. *J. Am. Chem. Soc.* **2007,** *129,* 14128–14129.
(5) Scott, J. C.; Bozano, L. D. *Adv. Mater.* **2007,** *19,* 1452–1463.
(6) Stikeman, A. *Technol. Rev.* **2002,** *105,* 31–31.
(7) Bandyopadhyay, A.; Pal, A. *J. Adv. Mater.* **2003,** *15,* 1949–1952.

(8) Möller, S.; Forrest, S. R.; Perlov, C.; Jackson, W.; Taussig, C. *J. Appl. Phys.* **2003,** *94,* 7811–7819.
(9) Tseng, R. J.; Huang, J. X.; Ouyang, J. Y.; Kaner, R. B.; Yang, Y. *Nano. Lett.* **2005,** *5,* 1077–1080.
(10) Chu, C. W.; Ouyang, J. Y.; Tseng, J. H.; Yang, Y. *Adv. Mater.* **2005,** *17,* 1440–1443.
(11) Kanwal, A.; Chhowalla, M. *Appl. Phys. Lett.* **2006,** *89,* 203103.
(12) Pradhan, B.; Batabyal, S. K.; Pal, A. J. *J. Phys. Chem. B* **2006,** *110,* 8274–8277.
(13) Lim, S. L.; Li, N. J.; Lu, J. M.; Ling, Q. D.; Zhu, C. X.; Kang, E. T.; Neoh, K. G. *ACS Appl. Mater. Interfaces* **2009,** *1,* 60–71.
(14) Ling, Q. D.; Liaw, D. J.; Zhu, C. X.; Chan, D. S. H.; Kang, E. T.; Neoh, K. G. *Prog. Polym. Sci.* **2008,** *33,* 917–978.
(15) Oh-e, M.; Asahi, T.; Masuhara, H. *J. Phys. Chem. B* **2002,** *106,* 5840–5844.

for applications in photovoltaics,[16,17] light-emitting diodes,[18,19] xerography,[20] and polymer memories.[21−24] On the other hand, oxadiazole-based polymers have been shown to be promising electron-transporting materials in light-emitting devices, due to their high electron affinity, as well as thermal, hydrolytic, and optical stability.[25,26] Materials containing oxadiazole electron-transporting segments have also been applied in electronic memory devices.[27,28] However, when bonded to stronger electron acceptors, such as maleimide and itaconimide, the oxadiazole groups can also act as electron donors.[29] Charge transfer (CT) interaction between the imide and oxadiazole groups is expected to be unstable, because of the small difference in electron affinities of these two moieties. Novel electrical switching behavior and volatile memory effects might be expected.[5] Thus, in this work, a solution-processable functional polyimide (P(BPPO)-PI, structure shown in Figure 1) containing 2,5-bis(4-phenoxyphenyl)-1,3,4-oxadiazole (BPPO) moieties as the electron donors and phthalimide (PI) moieties as the electron acceptors, was synthesized and characterized. Under an electric field, conformation-coupled CT occurred between the BPPO and PI moieties in a ITO/P(BPPO)-PI/Al sandwich device. The device is capable of exhibiting volatile bistable electrical switching characteristics of a static random access memory (SRAM). Molecular simulations of P(BPPO)-PI at both the ground and excited states (OFF and ON states of the device) were carried out to better understand the mechanism underlying the volatile switching phenomena.

2. Experimental Section

2.1. Instrumentation. FT-IR spectra of the synthesized monomers and polymers were recorded on a Perkin-Elmer GX FTIR spectrophotometer. ^{1}H NMR spectra were measured on a Bruker DRX-500 NMR spectrometer. Elemental analyses
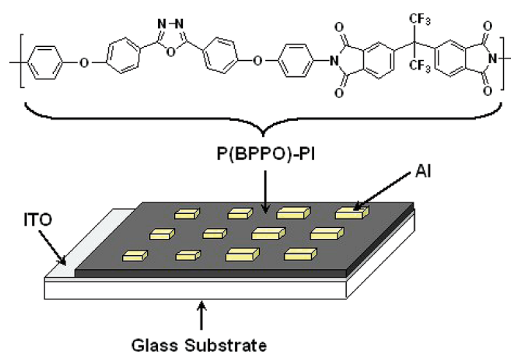

Figure 1. Molecular structure of P(BPPO)-PI and schematic diagram of the memory device consisting of a thin film of P(BPPO)-PI (∼50 nm) sandwiched between an ITO bottom electrode and an Al top electrode.

were carried out on a Perkin-Elmer 2400 elemental analyzer. The inherent viscosity of the polymer in *N,N*-dimethylacetamide (DMAc) was measured with an Ubbelohde viscometer. Thermogravimetric analysis (TGA) was conducted on a Perkin-Elmer Pyris 6 TGA thermogravimetric analyzer at a heating rate of 10 °C·min^{−1} and under a nitrogen or air flow rate of 20 cm[3] min^{−1}. The glass transition temperature (T_g) of the copolymer was measured on a Perkin-Elmer Pyris 6 differential scanning calorimeter (DSC) at a heating rate of 10 °C min^{−1} and under a nitrogen flow rate of 20 cm[3] min^{−1}. Weight average molecular weight (M_w) and number average molecular weight (M_n) were determined by gel permeation chromatography (GPC) on a Water GPC system equipped with four Waters Ultrastyragel columns (300 × 7.5 mm, guarded and packed with $1 × 10^5$, $1 × 10^4$, $1 × 10^3$, and 500 Å gels) in series. Tetrahydrofuran (THF, 1 mL min^{−1}) was used as the eluent and was monitored by a UV detector (JMST Systems, VUV-24, USA) at the wavelength of 254 nm. Monodispersed polystyrene was used as the molecular weight standard. UV−visible absorption and fluorescence spectra were measured on a Shimadzu UV-NIR 1601 spectrophotometer and Shimadzu RF 5301PC luminescence spectrophotometer, respectively. The thickness of P-(BPPO)-PI film cast on the indium−tin oxide (ITO) coated glass substrate was determined from the edge profile of the film, using the tapping mode, on a Veeco multimode atomic force microscope equipped with a Nanosensors PPP-NCHR silicon tip.

2.2. Reagents for Synthesis. *p*-Fluorobenzoic acid, aminophenol, potassium carbonate, and hydrazine monohydrate were purchased from Sigma-Aldrich Chemical Co., Acros Chemical Co., Showa Chemical Co., and Alfa Aesar Chemical Co., respectively, and were used as received. *N*-Methyl-2-pyrrolidinone (NMP), dimethyl sulfoxide (DMSO), and DMAc were purchased from Tedia Chemical Co. Tetrahydrofuran (THF) and *N,N*-dimethylformamide (DMF) were purchased from Echo Chemical Co. All the solvents were purified by distillation over calcium hydride and stored over 4 Å molecular sieves. Acetic anhydride and pyridine were purchased from Acros Chemical Co. and were used as received. 4,4′-Hexafluoroisopropylidenediphthalic anhydride (6FDA) was purchased from Chriskev Chemical Co. and was sublimed before use.

2.3. Synthesis of the Monomers and Copolymer. The synthesis routes for the monomers and polymer are illustrated in Figure 2. Details on their preparation and characterization are given below.

*Synthesis of 2,5-Bis(4-fluorophenyl)-1,3,4-oxadiazole (**BFOXD**).* 2,5-bis(4-fluorophenyl)-1,3,4-oxadiazole (BFOXD) was synthesized according to the published method.[30] After the reaction of

(16) Rumyantsev, B. M.; Berendyaev, V. I.; Tsegel'skaya, A. Yu.; Zhuravleva, T. S.; Klimenko, I. V. *Synth. Met.* **2005**, *152*, 85–88.
(17) Lozano, A. E.; Abajo, J.; Campa, J. G.; Guillén, C.; Herrero, J.; Gutiérrez, M. T. *J. Appl. Polym. Sci.* **2007**, *103*, 3491–3497.
(18) Shin, J. H.; Park, J. W.; Lee, W. K.; Jo, N. J.; Cho, W. J.; Ha, C. S. *Synth. Met.* **2003**, *137*, 1017–1018.
(19) Hsu, S. C.; Whang, W. T.; Chao, C. S. *Thin Solid Films* **2007**, *515*, 6943–6948.
(20) Wang, Z. Y.; Qi, Y.; Cao, J. P.; Sacripante, G. C.; Sundararajan, P. R.; Duff, J. D. *Macromolecules* **1998**, *31*, 2075–2079.
(21) Ling, Q. D.; Chang, F. C.; Song, Y.; Zhu, C. X.; Liaw, D. J.; Chan, D. S. H.; Kang, E. T.; Neoh, K. G. *J. Am. Chem. Soc.* **2006**, *128*, 8732–8733.
(22) Takimoto, K.; Kawade, H.; Kishi, E.; Yano, K.; Sakai, K.; Hatanaka, K.; Eguchi, K.; Nakagiri, T. *Appl. Phys. Lett.* **1992**, *61*, 3032–3−34.
(23) Cai, L.; Feng, M.; Guo, H. M.; Ji, W.; Du, S. X.; Chi, L. F.; Fuchs, H.; Gao, H. J. *J. Phys. Chem. C* **2008**, *112*, 17038–17041.
(24) Hahm, S. G.; Choi, S.; Hong, S. H.; Lee, T. J.; Park, S.; Kim, D. M.; Kwon, W. S.; Kim, K.; Kim, O.; Ree, M. *Adv. Funct. Mater.* **2008**, *18*, 3276–3282.
(25) Mikroyannidis, J. A.; Spiliopoulos, I. K.; Kasimis, T. S.; Kulkarni, A. P.; Jenekhe, S. A. *Maromolecules* **2003**, *36*, 9295–9302.
(26) Hughes, G.; Bryce, M. R. *J. Mater. Chem.* **2005**, *15*, 94–107.
(27) Pearson, C.; Ahn, J. H.; Mabrook, M. F.; Zeze, D. A.; Petty, M. C.; Kamtekar, K. T.; Wang, C. S.; Bryce, M. R.; Dimitrakis, P.; Tsoukalas, D. *Appl. Phys. Lett.* **2007**, *91*, 123506.
(28) Dimitrakis, P.; Normand, P.; Tsoukalas, D.; Pearson, C.; Ahn, J. H.; Mabrook, M. F.; Zeze, D. A.; Petty, M. C.; Kamtekar, K. T.; Wang, C. S.; Bryce, M. R.; Green, M. *J. Appl. Phys.* **2008**, *104*, 044510.
(29) Zhang, X.; Jin, Y. H.; Diao, H. X.; Du, F. S.; Li, Z. C.; Li, F. M. *Maromolecules* **2003**, *36*, 3115–3127.

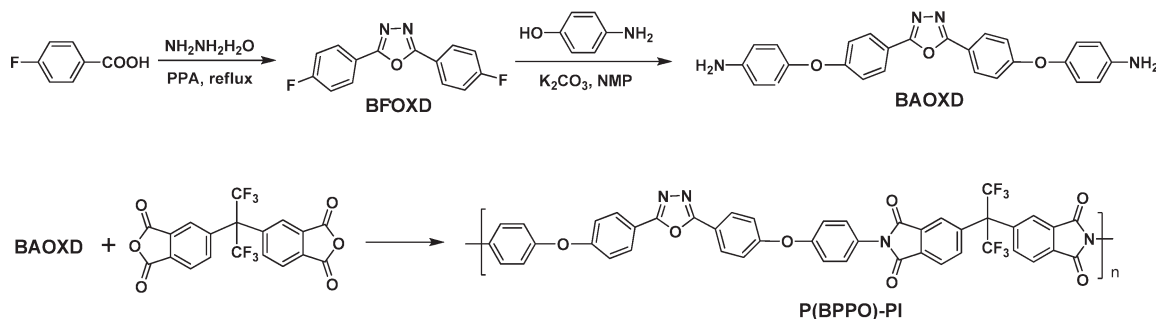(30) Hwang, S. W.; Chen, Y. *Polymer* **2000**, *41*, 6581–6587.

Figure 2. Synthesis Routes for the Monomers and P(BPPO)-PI.

p-fluorobenzoic acid (2 mol) and hydrazine hydrate (1 mol) in polyphosphoric acid (PPA), the mixture was recrystallized twice from ethanol, giving rise to small needlelike white crystals. FT-IR (KBr pellet): 1610 cm^{-1} ($-C=N-$). ^{1}H NMR (CDCl$_3$, 500 MHz), δ (ppm): 7.97–8.00 (m, 4H), 7.28–7.32 (t, $J = 8.87$ Hz, 4H).

Synthesis of 2,5-Bis(p-aminophenoxy-phenyl)-1,3,4-oxadiazole (BAOXD). BFOXD was reacted with 4-aminophenol and potassium carbonate in NMP at 150 °C, according to the method reported previously,[31] to produce the diamine. This method is based on the nucleophilic displacement of the activated fluoro-substituents by potassium phenoxide in polar aprotic solvent. FT-IR (KBr, pellet): 3454 and 3373 cm^{-1} (NH$_2$), 1612 cm^{-1} ($-C=N-$), 1240 cm^{-1} ($-O-$). ^{1}H NMR (d_6-DMSO, 500 MHz), δ (ppm): 8.01–8.03 (d, $J = 8.79$ Hz, 4H), 7.02–7.04 (d, $J = 8.79$ Hz, 4H), 6.82–6.84 (d, $J = 8.67$ Hz, 4H), 6.61–6.63 (d, $J = 8.71$ Hz, 4H), 5.08 (s, 4H).

Synthesis of the Copolymer (P(BPPO)-PI). 6FDA (0.509 g) was added slowly, with stirring, to 4 mL of DMAc containing 0.5 g of BAOXD at 0 °C. The mixture was stirred at ambient temperature for 24 h under a nitrogen atmosphere to form the poly(amic acid). Chemical imidization was carried out by adding 1 mL of acetic anhydride and 0.5 mL of pyridine into the poly(amic acid) solution, followed by heating the mixture at 140 °C for 6 h. The polymer solution was poured slowly into 300 mL of methanol with stirring. The precipitate was filtered, washed with methanol, and dried at 100 °C under reduced pressure. FTIR (film): 1784, 1724, 1376 cm^{-1} (imide). ^{1}H NMR (d_6-DMSO, 500 MHz), δ (ppm): 8.10–8.20 (6H), 7.95–7.98 (2H), 7.68–7.88 (2H), 7.45–7.58 (4H), 7.25–7.38 (8H).

2.4. Device Fabrication and Characterization. The indium–tin oxide (ITO, 200 nm in thickness) coated glass substrate was precleaned sequentially with deionized water, acetone and isopropanol by sonication for 15 min. A 100 μL DMAc solution of P(BPPO)-PI (10 mg·mL^{-1}) was spin-coated onto the ITO substrate at a rotation rate of 1500 rpm, followed by solvent removal in a vacuum chamber at 1×10^{-5} Torr and 60 °C for 10 h. The thickness of the polymer layer was about 50 nm, as determined by the AFM step profiling. Finally, an Al top electrode of about 400 nm in thickness was thermally deposited onto the polymer surface through a shadow mask at a pressure of about 1×10^{-7} Torr. Electrical property measurements were carried out on devices 0.4×0.4 mm^2, 0.2×0.2 mm^2, and 0.15×0.15 mm^2 in size, under ambient conditions, using an Agilent 4155C semiconductor parameter analyzer equipped with an Agilent 41501B pulse generator. The current density–voltage ($J-V$) data reported were based on device units of 0.4×0.4 mm^2 in size, unless stated otherwise. ITO was maintained as the ground electrode during the electrical measurements.

2.5. Molecular Simulation. Molecular simulations of P-(BPPO)-PI were carried out with the Gaussian 03 (Revision E. 01) program package on an Intel Xeon EM64T workstation. The calculations for the ground and excited states were carried out with 1 CPU and 2GByte memory, and 4 CPUs and 8GByte memory, respectively. Electronic properties of P(BPPO)-PI at the ground state, including molecular orbitals, electrostatic potential (ESP) surface, and dipole moment, were calculated from the density function theory (DFT), using the Becke's three-parameter functional with the Lee, Yang, and Parr correlation functional method (B3LYP) and the basis set 6-31G with d function added to heavy atoms (in short, DFT B3LYP/6-31G(d)).[32] On the basis of the ground state optimized geometry, the optimized geometry, dipole moment, and ESP surface of the first excited state were calculated with configuration interaction involving single electron excitations (CIS) method.[33] For both molecular simulations, vibrational frequencies were calculated analytically to ensure that the optimized geometries really correspond to the total energy minima.

3. Results and Discussion

3.1. Characterization of the Functional Polyimide, P(BPPO)-PI. P(BPPO)-PI exhibits good solubility in common solvents, such as THF, DMAc, NMP, and DMF, at room temperature. It can be cast into transparent and uniform films from solutions by spin-coating. The inherent viscosity of P(BPPO)-PI in DMAc (0.5 g L^{-1}) is 0.35 g dL^{-1}, as measured by the Ubbelohde viscometer. The M_n and M_w of the copolymer are 6.6×10^4 and 9.5×10^4, respectively, and thus a polydispersity index of 1.44, as determined by GPC. The copolymer exhibits a glass transition temperature (T_g) of about 250 °C and 5 and 10% weight loss at 545 and 566 °C, respectively, in nitrogen.

Figure 3 shows the UV–visible absorption spectra of P(BPPO)-PI, as well as the 6FDA and BAOXD monomers, in DMAc. The concentration of P(BPPO)-PI was about 5×10^{-7} mol L^{-1}. The concentrations of 6FDA and BAOXD were adjusted to be comparable to that of the repeat units of P(BPPO)-PI in the solution. The absorption spectra were cut off at 262 nm because of strong interference of the solvent in the short wavelength region. As shown in Figure 3, P(BPPO)-PI exhibits a maximum

(31) Hamciuc, E.; Hamciuc, C.; Cazacu, M. *Eur. Polym. J.* **2007**, *43*, 4739–4749.

(32) Frisch, M. J.; Trucks, G. W.; Schlegel, H. B.; Scuseria, G. E.; Robb, M. A.; Cheeseman, J. R.; Montgomery, Jr., J. A.; Vreven, T.; Kudin, K. N.; Burant, J. C. et al. Gaussian 03 (Revision E. 01); Gaussian, Inc.: Wallingford, CT, 2008.

(33) Foresman, J. B.; Head-Gordon, M.; Pople, J. A.; Frisch, M. J. *J. Phys. Chem.* **1992**, *96*, 135–149.
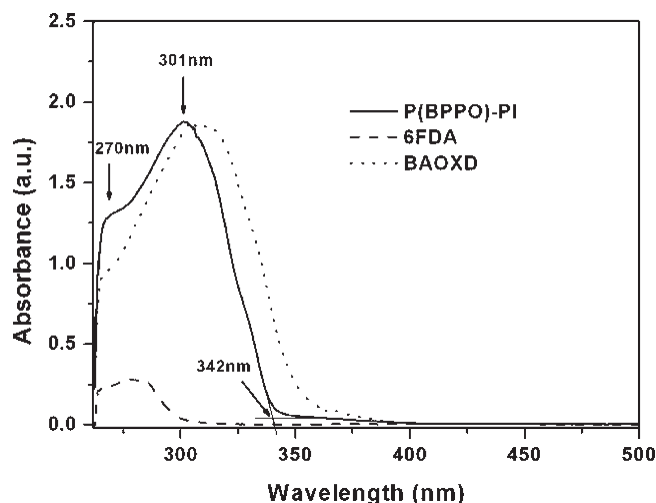
Figure 3. UV−visible absorption spectra of P(BPPO)-PI, as well as of the two monomers 6FDA and BAOXD, in DMAc solution. The concentration of P(BPPO)-PI is about 5×10^{-7} mol L^{-1}. The concentrations of 6FDA and BAOXD were adjusted to be comparable to that of the repeat units of P(BPPO)-PI in the solution. The absorption spectrum of the BAOXD monomer was normalized to the maximum absorption peak of P-(BPPO)-PI at 301 nm for ease of comparison.

absorption peak at 301 nm, which can be attributed to the $\pi \rightarrow \pi^*$ transition of the π electronic system delocalized along the 2,5-bis(4-phenoxyphenyl)-1,3,4-oxadiazole (BPPO) moieties.[34,35] The weak absorption peak at 270 nm originates from the combined absorptions of the PI moieties and the benzene rings of the BPPO moieties.[34,36] The absorption edge of P(BPPO)-PI extends to about 342 nm, from which the band gap of this copolymer is estimated to be 3.6 eV. The absorption spectrum of the BAOXD monomer is normalized to the maximum absorption peak of P(BPPO)-PI at 301 nm for ease of comparison. The spectral lineshapes of P(BPPO)-PI and BAOXD in the long wavelength region are similar, except that the absorption spectrum of P(BPPO)-PI has blue-shifted by about 10 nm. This blue-shift is probably induced by the strong electron-withdrawing (acceptor) property of the imide groups in P(BPPO)-PI.[37]

Figure 4 shows the photoluminescence (PL) spectrum of P(BPPO)-PI, as well as those of the two oxadiazole monomers, BFOXD and BAOXD, in DMAc. The concentration of P(BPPO)-PI solution for the PL measurement was about 10^{-8} mol L^{-1}. The concentrations of BFOXD and BAOXD were adjusted to be comparable to that of the repeat units of P(BPPO)-PI in the solution. All the emission spectra were obtained with the excitation wavelength of 280 nm. As shown in Figure 4, BFOXD exhibits an intense emission peak at 346 nm, similar to that of 2,5-diphenyl-1,3,4-oxadiazole at 349 nm reported previously,[35] consistent with the fact that oxadiazole
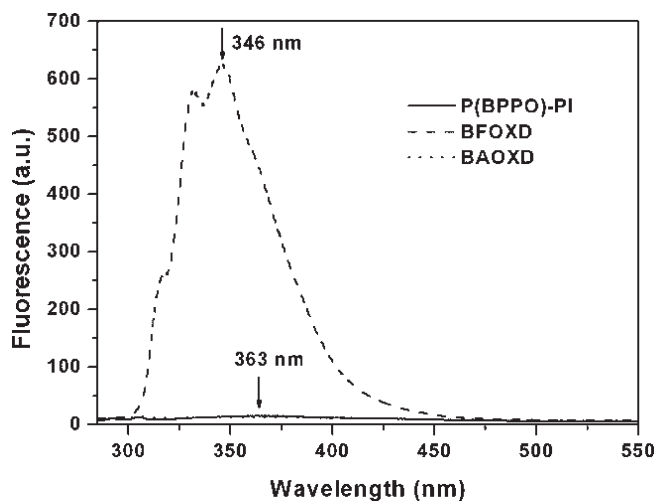

Figure 4. Fluorescence emission spectra of P(BPPO)-PI, as well as of the two oxadiazole monomers BFOXD and BAOXD, in DMAc solution. The concentration of P(BPPO)-PI is about 1×10^{-8} mol L^{-1}. The concentrations of BFOXD and BAOXD were adjusted to be comparable to that of the repeat units of P(BPPO)-PI in the solution. All the emission spectra were obtained with the excitation wavelength of 280 nm.

derivatives are efficient fluorescence chromophores.[38] In comparison to BFOXD, the fluorescence of P(BPPO)-PI is significantly quenched, indicating considerable decay of the excited singlet state of oxadiazole moieties, either by charge or energy transfer between the oxadiazole and phthalimide moieties.[39,40] The poor match between the emission spectrum of BFOXD and the absorption spectrum of 6FDA rules out the possibility of energy transfer.[41] As the electron affinity of 2,5-diphenyl-1,3,4-oxadiazole (0.449 eV)[42] is lower than that of phthalimide (1.01 eV),[43] the oxadiazole moieties can act as electron donors in the copolymer, although they have been widely employed as the electron-accepting chromophores in the electroluminescence devices.[44] Thus, electrons are transferred from the oxadiazole to phthalimide moieties, accounting for the observed fluorescence quenching in P-(BPPO)-PI. This donor−acceptor interaction process will be studied further by molecular simulation (see below).

In addition, the fluorescence is almost completely quenched in the monomer BAOXD. In comparison to 2,5-diphenyl-1,3,4-oxadiazole, which gives rise to intense fluorescence, BAOXD contains two additional groups, viz., phenoxyl and amine groups, indicating that fluorescence quenching in BAOXD probably have originated from these two groups. As reported previously,[45,46] 2,5-bis(4-phenoxyphenyl)-1,3,4-oxadiazole gives rise to intense emission at 358 nm, suggesting that the phenoxyl group in BAOXD does not quench the fluorescence. Thus, the amine groups are probably responsible for

(34) Wolarz, E.; Chrzumnicka, E.; Fischer, T.; Stumpe, J. *Dyes. Pigments.* **2007**, *75*, 753–760.
(35) Franco, O.; Orgzall, I.; Regenstein, W.; Schulz, B. *J. Phys.: Condens. Matter.* **2006**, *18*, 1459–1472.
(36) Xu, S. G.; Yang, M. J.; Gao, S. K. *Polymer* **2007**, *48*, 2241–2249.
(37) Liu, C. B.; Zhao, P.; Huang, W. *Cent. Eur. J. Chem.* **2007**, *5*, 303–315.
(38) Wang, C. S.; Pålsson, L. O.; Batsanov, A. S.; Bryce, M. R. *J. Am. Chem. Soc.* **2006**, *128*, 3789–3799.

(39) Shibano, Y.; Umeyama, T.; Matano, Y.; Tkachenko, N. V.; Lemmetyinen, H.; Imahori, H. *Org. Lett.* **2006**, *8*, 4425–4428.
(40) Lukas, A. S.; Zhao, Y. Y.; Miller, S. E.; Wasielewski, M. R. *J. Phys. Chem. B.* **2002**, *106*, 1299–1306.
(41) Gómez, R.; Segura, J. L.; Martín, N. *Org. Lett.* **2005**, *7*, 717–720.
(42) Lami, H.; Laustriat, G. *J. Chem. Phys.* **1968**, *48*, 1832–1840.
(43) Paul, G.; Kebarle, P. *J. Am. Chem. Soc.* **1989**, *111*, 464–470.
(44) Schulz, B.; Bruma, M.; Brehmer, L. *Adv. Mater.* **1997**, *9*, 601–613.
(45) Yu, Y. H.; Chen, Y. *J. Polym. Sci. Part A: Pol. Chem.* **2003**, *41*, 2765–2777.
(46) Chen, Y.; Hwang, S. W.; Yu, Y. H. *Polymer* **2003**, *44*, 3827–3835.

quenching the fluorescence in BAOXD. The assumption is supported by the quenching of fluorescence in oxadiazole derivatives by electron donors, such as N,N'-dimethylaniline, through CT interaction.[47,48] As the phenoxyl group is able to transmit the substituent effect,[49] it can act as a mediator to facilitate the electron transfer from the amine group to the oxadiazole group in the BAOXD monomer. Similar mediation effect by the phenoxyl group probably also exists in P(BPPO)-PI to facilitate CT interaction between the oxadiazole and phthalimide moieties.

3.2. Electrical Switching Effects and Memory Performance of the ITO/P(BPPO)-PI/Al Device. The current density−voltage (J−V) characteristics of an ITO/P-(BPPO)-PI/Al sandwich device are shown in Figure 5a. During the first positive sweep from 0 to 4 V (with Al as the anode and ITO as the cathode), the device was initially in the low-conductivity (OFF) state and switched to the high-conductivity (ON) state at 2.3 V, with an ON/OFF current ratio in the order of 1×10^4. The device remained in the ON state when the positive voltage sweep was repeated (the second sweep). The memory device cannot be reset to the initial OFF state by the application of a reverse sweep (the third sweep) and is thus nonerasable. The ON state can be retained for a period of about 4 min after turning off the power, after which the device relaxed back to the OFF state, indicating the "remanent", yet volatile, nature of the ON state. The device can be switched to the ON state again when the reverse threshold voltage was applied (−2.5 V in the fourth sweep). It remained in the ON state when the negative sweep was repeated (the fifth sweep). The results suggest that the P-(BPPO)-PI device can be written bidirectionally at positive and negative threshold voltages of comparable magnitude. The sixth sweep was conducted about 4 min after turning off the power. The device was found to have relaxed to the OFF state again without any erasing process. The ON state can be reprogrammed when the reverse threshold voltage (−2.4 V in the sixth sweep) was reapplied. The volatile ON state can be electrically sustained either by a refreshing voltage pulse of −1 V (1 ms duration) in every 5 s (the "rf" trace in Figure 5a) or a continuous bias of −1 V (Figure 5b). Figure 5b also shows the effect of operation time on the stability of the P-(BPPO)-PI device. Under a constant stress of −1 V, no obvious degradation in current density is observed for both the ON and OFF states over a 5 h period. In addition, the ON and OFF state are also stable up to 1×10^8 read pulses of −1 V, as shown in Figure 5c. The "remanent", yet volatile, nature of the ON state, as well as the randomly accessible ON and OFF states in each ITO/P(BPPO)-PI/Al device, are similar to the data remanence behavior of a static random access memory (SRAM). In a SRAM, the memory can be written into or read from
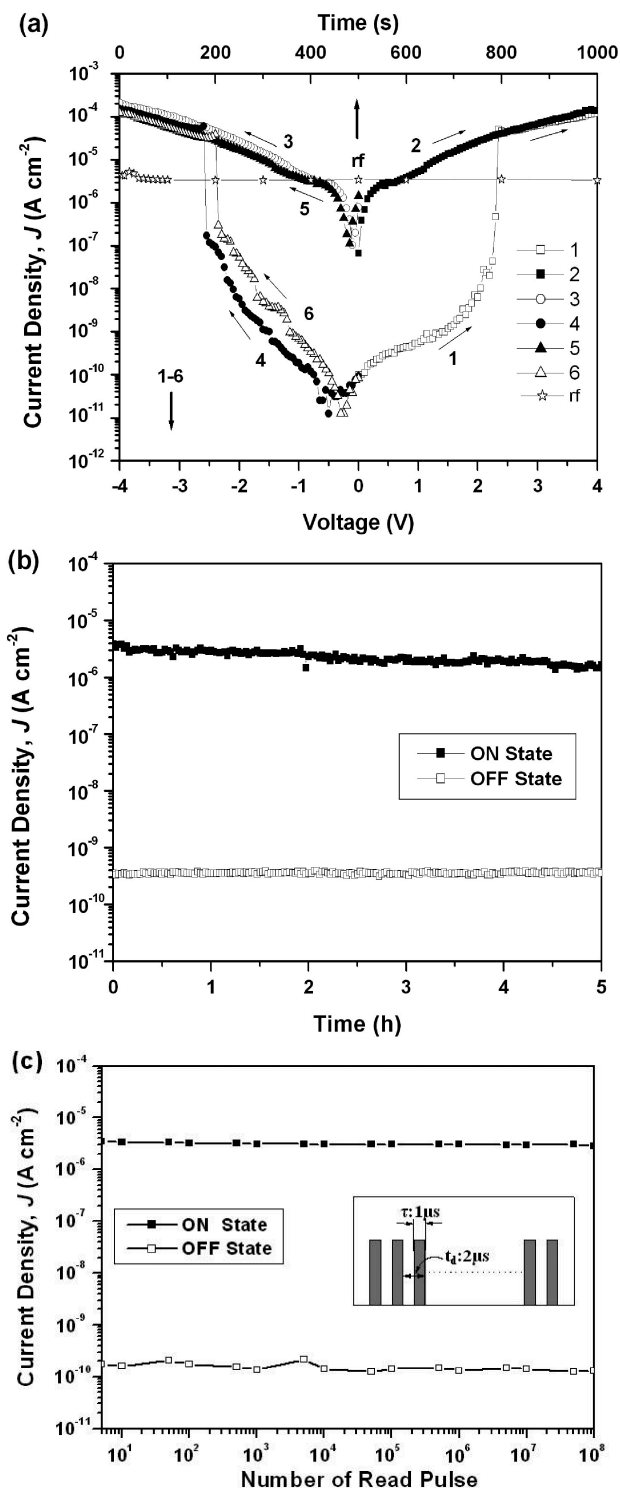

Figure 5. (a) Current density−voltage (J−V) characteristics of a 0.4×0.4 mm² ITO/P(BPPO)-PI/Al device. The sequence and direction of each sweep are indicated by the respective number and arrow. The fourth and sixth sweeps were conducted about 4 min after turning off the power. The ON state was sustained by a refreshing voltage pulse of −1 V (pulse duration = 1 ms) in every 5 s, as shown by the "rf" trace. (b) Effect of operation time on the ON and OFF states of the ITO/P(BPPO)-PI/Al device under a constant stress of −1 V. (c) Effect of read pulse of −1 V on the ON and OFF states of the ITO/P(BPPO)-PI/Al device. The inset shows the pulse used for the measurement.

(47) Feng, L. H.; Chen, Z. B.; Bai, F. L. *Spectrochim. Acta, A* **2004**, *60*, 3029–3032.
(48) Feng, L. H.; Chen, Z. B. *Spectrochim. Acta, A* **2006**, *63*, 15–20.
(49) Huang, W.; Zhang, X.; Ma, L. H.; Wang, C. J.; Jiang, Y. B. *Chem. Phys. Lett.* **2002**, *352*, 401–407.

in any order, regardless of the memory location last accessed, and the stored data are retained temporarily after the power has been turned off. The memory,
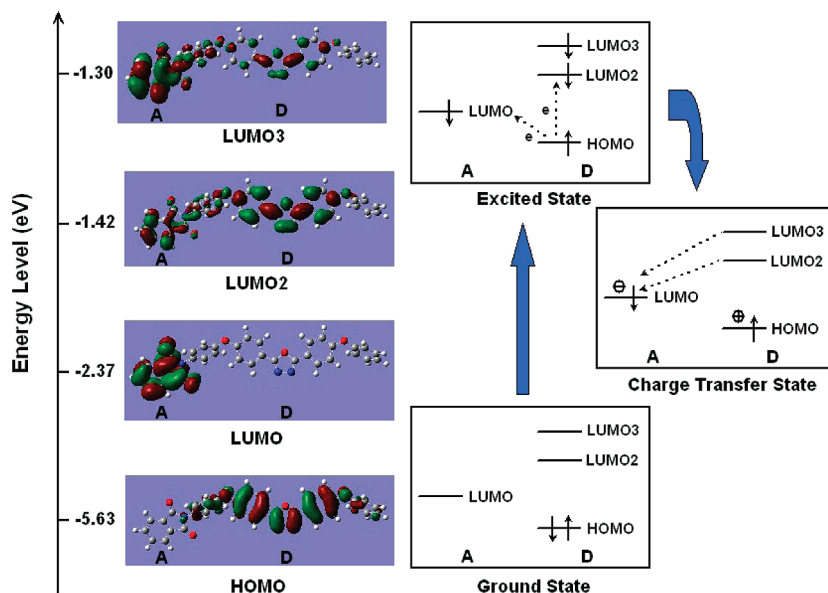
Figure 6. Calculated molecular orbitals, the corresponding energy levels of the basic unit (BU), and the plausible electronic transitions under an electric field.

however, is volatile and the data are eventually lost when the memory remains in the power-off state.

The $J-V$ characteristics are found to have good reproducibility, except for the slight variations in switching threshold voltages associated with conformational relaxation of the polymer chain. In addition, devices with different active areas of $0.4 \times 0.4\,mm^2$, $0.2 \times 0.2\,mm^2$, and $0.15 \times 0.15\,mm^2$ show almost the same $J-V$ characteristics, indicating that the current density is independent of the device areas. The SRAM switching behavior for different device units, as well as for each device size/configuration, can be reproduced with good accuracy. The volatile ON state, good reproducibility, and area-independent current density rule out the possibility of filament effect,[50] metal diffusion,[51] and dielectric breakdown in the present devices.

3.3. Switching Mechanism. To better understand the switching behavior of the P(BPPO)-PI memory device, we studied the electronic properties of P(BPPO)-PI at the ground state by density function theory (DFT). Calculations of the molecular orbitals, dipole moment, and ESP surfaces of the basic units (BU), taking into account both functional moieties, viz., the PI and BPPO moieties, were carried out at the B3LYP/6-31G(d) level with the Gaussian 03 program package.[32] The trifluoromethyl groups of P(BPPO)-PI were not included in the calculation because they probably do not significantly affect the electronic properties of the BU.[52] The highest occupied molecular orbital (HOMO) and lowest unoccupied molecular orbital (LUMO) of the BU, as well as the plausible electronic transitions under excitations, are demonstrated in Figure 6. The HOMO is located mainly on the BPPO moieties, whereas the first LUMO is located on the PI moieties, indicating that in the copolymer, the BPPO

moieties act as the electron donors and the PI moieties act as the electron acceptors. In addition, the two higher excited energy levels (LUMO2 and LUMO3) are distributed over all the BU. Under excitations with sufficient energy, electrons in the ground state of P(BPPO)-PI can transit to the various excited states.

When the applied electric field reaches the switch-on voltage, some electrons at the HOMO of P(BPPO)-PI accumulate sufficient energy and transit to the LUMO2 and LUMO3, because of overlapping of the HOMO with these LUMOs at the oxadiazole moieties, to result in an excited state. As the LUMO2 and LUMO3 are distributed over the entire BU, the excited electrons on the oxadiazole moieties can delocalize readily to the phthalimide moieties, which has a higher electron affinity and where they can relax to the lowest excited singlet state via internal conversion. As a result, CT between BPPO and PI can occur. This CT process is supported by the significant quenching of fluorescence in P(BPPO)-PI, as shown in Figure 4. In addition to the indirect CT process, CT can also occur via direct electron transition from the HOMO to the LUMO. Under the electric field, the generated holes at the HOMO can delocalize to the conjugated oxadiazole moieties, giving rise to an open channel for the charge carriers (holes) to migrate through. Thus, the current density increases rapidly and the P(BPPO)-PI device switches to the high-conductivity (ON) state. Although the oxadiazole derivatives are widely used as electron-transporting materials in electroluminescence devices, they do not possess high hole-blocking properties.[53] It is reported that holes can migrate successfully through a 2-(4-biphenylyl)-5-(4-*tert*-butylphenyl)-1,3,4-oxadiazole (PBD) film with thickness as high as 30 nm.[54] Thus, it is reasonable

(50) Henish, H. K.; Smith, W. R. *Appl. Phys. Lett.* **1974**, *24*, 589–591.
(51) Lim, S. L.; Tan, K. L.; Kang, E. T. *Langmuir* **1998**, *14*, 5305–5313.
(52) LaFemina, J. P. *Chem. Phys. Lett.* **1989**, *159*, 307–309.
(53) Kido, J.; Hayase, H.; Hongawa, K.; Nagai, K.; Okuyama, K. *Appl. Phys. Lett.* **1994**, *65*, 2124–2126.
(54) Kido, J.; Ohtaki, C.; Hongawa, K.; Okuyama, K.; Nagai, K. *Jpn. J. Appl. Phys.* **1993**, *32*, L917–L920.

that the BPPO moieties in P(BPPO)-PI can act as a hole-transporting pathway, albeit not as efficient as some of the strong electron donor species. As the P(BPPO)-PI chains are nonconjugated, charge carriers probably do not move along the copolymer backbone. Instead, they probably hop between neighboring oxadiazole moieties (either in the same or neighboring copolymer chains).

In a ring-containing organic molecule, the torsional angle between two aromatic moieties will increase under a static electric field, resulting in an enhanced potential energy barrier for the intramolecular CT.[55] Thus, the conformation of the molecule will change from one in which electrons can flow easily to one in which this flow is restrained. As the conformational change normally lags behind the CT process, when an electric field is applied to the P(BPPO)-PI device, electrons are transferred from the oxadiazole donors to the phthalimide acceptors via the phenoxyl mediator.[49] Thereafter, conformational changes can result in increased torsional displacement between the oxadiazole and phthalimide moieties, producing a potential barrier for the back electron transfer. As a result, the conductive CT states can be sustained, and the high-conductivity (ON) state is retained. Once the conductive CT states are formed under an applied electric field, they facilitate electrical conduction under both biases and the device cannot be switched off by applying a reverse bias of the same magnitude. Nevertheless, the polymer relaxes to its original conformation sometime after removal of the applied electric field. The potential barrier disappears, and the CT states dissociate via back electron transfer from the phthalimide moiety to the oxadiazole moiety. Volatile electrical switching behavior is thus observed. The OFF-ON switching associated with the field-induced formation of conductive CT states in P-(BPPO)-PI is also consistent with the fact that the device can be written bidirectionally at positive and negative threshold voltages of about the same magnitude (Figure 5a).

To elucidate the above CT and conformational change processes experimentally, we studied the UV−visible absorption spectrum of the solid state P(BPPO)-PI film with and without the applied electric field. A liquid Hg droplet was employed as the top electrode in place of the Al contact. After an electrical sweep from 0 to −4 V (with ITO as the ground electrode), the Hg electrode was removed and the resultant UV−visible absorption spectrum was compared with the pristine spectrum before the electrical sweep. In Figure 7, OFF-1, ON-1, and OFF-2 denote, respectively, the absorption spectra of P(BPPO)-PI film spin-coated on ITO substrate measured before, immediately after, and 3 h after the electrical sweep. The P(BPPO)-PI film was found to exhibit a broad absorption band between 500 and 700 nm and an absorption shoulder at 360 nm (OFF-1 spectrum), which are
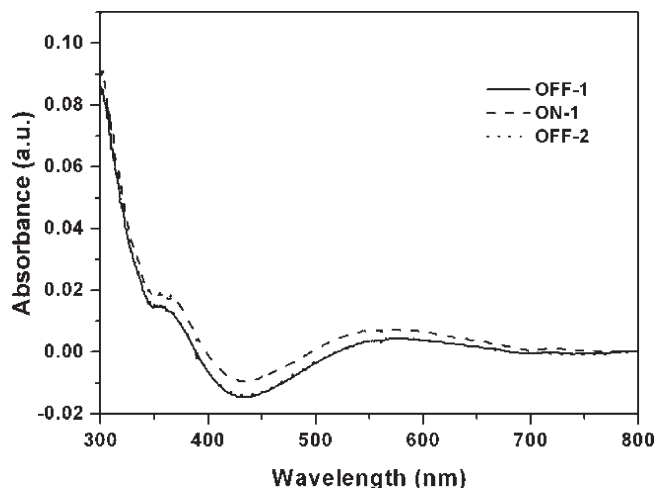

Figure 7. UV−visible absorption spectra of P(BPPO)-PI film spin-coated on ITO substrate. OFF-1, ON-1, and OFF-2 denote, respectively, the absorption spectra of P(BPPO)-PI films measured before, immediately after, and 3 h after an electrical sweep (0 to −4 V, with a removable Hg droplet as the cathode and ITO as the anode).

associated, respectively, with the absorption of CT complexes in the ground state[56] and the formation of $\pi-\pi$ stacks of the oxadiazole units.[57,58] Upon excitation by an applied electric field, the intensities of both absorption bands are enhanced (ON-1 spectrum). The increase in intensity of the CT absorption band is consistent with an increase in concentration of the CT state, arising from the conformation-coupled CT induced by the applied electric field. The increase in concentration of the conductive CT state leads to the switching of the P(BPPO)-PI device from the OFF state to the ON state. Because of CT from the oxadiazole donors to the phthalimide acceptors, the oxadiazole groups become positively charged. Driven by the applied electric field, the charged oxadiazole groups have the tendency to interact with the neighboring neutral oxadiazole groups, forming the partial or full face-to-face conformation.[59] Thus, the $\pi-\pi$ stacking of the oxadiazole groups is enhanced, as indicated by the increase in intensity of the absorption shoulder at about 360 nm. The increased extent of face-to-face conformation of the conjugated oxadiazole groups also facilitates the migration of charge carriers and sustains the ON state. Sometime after removal of the electric field, the conformation of the polymer chain relaxes to its initial state and the induced intramolecular CT disappears. Thus, the concentration of CT complexes decreases to the initial level due to the back electron transfer, and the extent of face-to-face conformation of the oxadiazole moieties also relaxes to the initial level. As a result, the original OFF-state absorption spectrum is recovered (OFF-2 spectrum). The effect of applied electric field on the absorption spectrum of P(BPPO)-PI film provides further support to the conformation-coupled CT process in P(BPPO)-PI. The CT

(55) Cacelli, I.; Ferretti, A.; Girlanda, M.; Macucci, M. *Chem. Phys.* **2006**, *320*, 84–94.
(56) Benson-Smith, J. J.; Goris, L.; Vandewal, K.; Haenen, K.; Manca, J. V.; Vanderzande, D.; Bradley, D. D. C.; Nelson, J. *Adv. Funct. Mater.* **2007**, *17*, 451–457.

(57) Lee, R. H.; Hsu, H. F.; Chan, L. H.; Chen, C. T. *Polymer* **2006**, *47*, 7001–7012.
(58) Paul, P. K.; Hussain, S. A.; Bhattacharjee, D. *J. Lumin.* **2008**, *128*, 41–50.
(59) Teo, E. Y. H.; Ling, Q. D.; Song, Y.; Tan, Y. P.; Wang, W.; Kang, E. T.; Chan, D. S. H.; Zhu, C. X. *Org. Electron.* **2006**, *7*, 173–180.
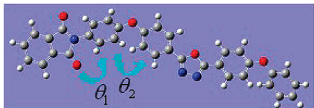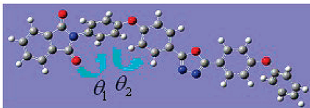
Properties	Ground State	Excited State
Dipole Moment	2.82 Debye	3.06 Debye
ESP Surface		
Optimized Geometry		
Dihedral Angle	$\theta_1 = 40.1°$, $\theta_2 = 67.1°$	$\theta_1 = 54.6°$, $\theta_2 = 72.7°$

Figure 8. Dipole moments, electrostatic potential (ESP) surfaces, optimized geometries of P(BPPO)-PI, and dihedral angles between the component aromatic moieties at the ground and excited states. For the ESP surfaces, the positive ESP regions are in red, whereas the negative ESP regions are in blue. For the optimized geometries, the dihedral angle between the phthalimide plane and the phenoxyl plane is indicated by θ_1, and the dihedral angle between the phenoxyl plane and the oxadiazole plane is indicated by θ_2.

absorption band is located at around 560 nm, indicating that the CT process occurs with the highest probability at about 2.2 eV. This energy value is comparable to the switching threshold voltage (~ 2.3 V) in the $J-V$ characteristics, consistent with a threshold voltage-induced CT process.

Molecular simulation of the excited state of P(BPPO)-PI was carried out to further demonstrate the conformation-coupled CT process. Optimized geometry, electrostatic potential (ESP) surface, and dipole moment of the BU at excited state were studied at the CIS/6-31G (d) level with the Gaussian 03 program package. The corresponding electronic properties of BU at ground state were employed as the reference. Figure 8 summarizes the molecular simulation results of both the ground and excited states. From the ESP surfaces, it can be seen that P(BPPO)-PI at both states consist mainly of positive ESP region, with some minor negative ESP regions arising from the sp^2 hybridized O atoms in the phthalimide group and sp^2 hybridized N atoms in the oxadiazole group. As ESP is the potential energy of a proton at a particular location of a molecule, it can reflect the local electron density. Accordingly, the negative ESP regions in P(BPPO)-PI suggest concentrated local electron densities near the sp^2 hybridized atoms that possess certain electron-withdrawing capability. In comparison with P(BPPO)-PI at the ground state, P(BPPO)-PI at the excited state exhibits larger negative regions around the O atoms in the phthalimide group, indicating that under excitation, electron will transfer to the phthalimide moiety from other moieties in the molecule. This electronic process is consistent with the electric field induced electron transfer process from the oxadiazole moieties to the phthalimide moieties, as mentioned above. The electron transfer process is also supported by the enhanced dipole moment of P(BPPO)-PI at the excited state (3.06 D) in comparison to that at the ground state (2.82 D).

Following the electron transfer process, the conformation of P(BPPO)-PI molecule also undergoes changes under the applied electric field, as indicated by the difference in optimized geometries of P(BPPO)-PI at the ground and excited states. The dihedral angle between the phthalimide plane and the phenoxyl plane (θ_1) increases from 40.1 to 54.6°, and the dihedral angle between the phenoxyl plane and the oxadiazole plane (θ_2) increases from 67.1 to 72.7°. The enhanced dihedral angles are consistent with the previous report on the increase in torsional angle induced by a static electric field applied perpendicular to the ring-to-ring linkage.[55] The torsional conformation at the excited state reduces the effective conjugation of the π electrons between neighboring aromatic moieties, and generate an intramolecular potential barrier which prevents the back transfer of charges. As a result, the conductive CT state (ON state) is sustained, and cannot be dissociated by a reverse bias without the accompanied conformation relaxation.

After removal of the electric field, the P(BPPO)-PI molecule tends to relax to its initial conformation. The dihedral angles between the component aromatic moieties decrease to their initial levels and the potential barriers disappear, making the back electron transfer feasible.[55] Also, as determined from the molecular simulation results, the dipole moment of P(BPPO)-PI in the excited state is only 3.06 D, which is probably not high enough to retain the conductive CT states. As a result, the conductive CT states are not stable and dissociate after sometime upon removal of the electric field, resulting in the eventual loss of the ON state and the volatile nature of the memory effect.

In comparison with the more rigid functional polyimide containing triphenylamine and phthalimide moieties (TP6F−PI, $T_g = 316$ °C) which exhibits dynamic random access memory (DRAM) behavior arising predominantly from unstable CT states,[21] the present P(BPPO)-PI has a lower T_g (250 °C), a more flexible chain and can undergo conformational changes more readily under an electric field. As analyzed above, the conductive CT states of P(BPPO)-PI are difficult to dissociate by a reverse bias, due to the potential barrier for back electron transfer induced by the conformational change. Therefore, the device based on P(BPPO)-PI exhibits data "remanence" (temporary retention) of a SRAM, differing from the volatile DRAM effect of

the device based on TP6F−PI, upon removal of the power supply.

4. Conclusions

A solution-processable functional polyimide, P-(BPPO)-PI, containing oxadiazole and phthalimide moieties, was synthesized. During electrical sweeps, devices based on the ITO/P(BPPO)-PI/Al sandwich structure exhibit volatile bistable electrical switching characteristics of a static random access memory (SRAM). As elucidated from the molecular simulation results, the oxadiazole moieties can act as the electron donors in the presence of phthalimide moieties of higher electron affinity. Electric field-induced charge transfer (CT) from the oxadiazole donor to the phthalimide acceptor gives rise to a conductive CT state, which accounts for the transition of the P(BPPO)-PI device from the OFF state to the ON state. The accompanied conformational change induced by the electric field gives rise to a potential barrier for the back transfer of electrons, leading to the "remanence" (temporary retention) of the ON state. As the small dipole moment of P(BPPO)-PI in the ON state probably cannot retain the conformation-coupled CT state in the absence of an applied field, the ON state is volatile in nature and is eventually lost when the memory is not powered. The conformation-coupled CT mechanism was further elucidated from the molecular simulations of P(BPPO)-PI in the ground and excited states, and the changes in photoelectronic spectra of P(BPPO)-PI film in the presence and absence of an applied electric field (or in the ON and OFF states).